Journal of Immunology and Infectious Diseases
Volume 8 | Issue 1
ISSN: 2394-6512

Research Article Open Access

Close Packing of Elements of Transparent Metamaterials in UVC Diapason and its Influence on The Decontamination Efficiency

Enaki NA*, Starodub E, Paslari T, Turcan M and Bazgan S

Quantum Optics and Kinetic Processes Laboratory, Institute of Applied Physics, Ministry of Education, Culture and Research, Republic of Moldova, Academiei str. 5, Chisinau, R. Moldova

***Corresponding author:** Enaki NA, Quantum Optics and Kinetic Processes Laboratory, Institute of Applied Physics, Ministry of Education, Culture and Research, Republic of Moldova, Academiei str. 5, Chisinau, R. Moldova, Tel: +37322743351, E-mail: enakinicolae@yahoo.com

Citation: Enaki NA, Starodub E, Paslari T, Turcan M, Bazgan S (2021) Close Packing of Elements of Transparent Metamaterials in UVC Diapason and its Influence on The Decontamination Efficiency. J Immunol Infect Dis 8(1): 104

Abstract

A new method for repacking optical metamaterials formed from fiber or spherical elements of various diameters is proposed for ultraviolet C (UVC) decontamination of infected liquids that flow between these elements. It is proposed the method of repacking of metamaterial formed from closed packing big fibers/spheres with other subsystems of thin fibers/bubbles replaced in the free space between the first packing fibers/spheres. This method of the repacking of quasi-periodic metamaterials gives us the possibility to increase the total contact surface of the quarts spheres/fibers with contaminated fluids (water, aerosols). The repacking procedure may be continued by introducing other subsystems of small spheres or thin fibers in the repacked material. This approach opens the attractive possibilities for their use both in decontamination fluids and in the manipulating of pathogens in the special zones. The new equipment works on the above principle that using UVC sources for decontamination of pathogens (viruses and bacteria).

Keywords: Medical Optics and Biotechnology; Close Packing of Fiber/Spheres; Evanescent Zone of UVC Radiation; Contact Surface with Pathogens; Decontamination/Desinfection Rate

Introduction

In this pandemic period, it is important to identify the possibilities to increase the efficiency of the decontamination rate of fluids (aerosols, water, blood, blood plasma, etc) under the action of electromagnetic ultraviolet C radiation (UVC), defined in spectral range of wavelengths, $200-280\,nm$ (see for example Ref. [1]). Recently a big number of Refs. [2-5] proposed to the UVC radiation for decontamination of fluids and surfaces in order to inactivate pathogens (bacteria and viruses) like COVID-19 [2-5]. In comparison with these studies, this paper proposes to apply variously geometry of packing elements of composite metamaterials like photon crystal in order to substantially improve the decontamination rate. To use the optical fibres and other optical elements in order to manipulate the UVC radiation was the subject of many recent investigations [6-20]. This paper is focused to develop the idea of the fabrication of composite metamaterials from micro- to nano- levels using the optical contact between synthesized metamaterial elements with various structural dimensions. Here it is proposed to use both decontamination fluids and in the actual handling of pathogens to combine thick and thin elements of composite metamaterials constructed from spheres or optical fibre transparent in UVC spectral range of energies, $4.43-6.2\ \mathrm{eV}$, in order to achieve the expected results in decontamination efficiency.

To improve the contact surface between the pathogens and UVC radiation, we proposed the new more compact decontamination equipment for liquids and gases based on the idea of repacking big and small elements into optical materials. This communication proposes to close packing big and small elements of metamaterial in order to achieve both the deeper penetration of UVC radiation inside the translucent fluids and improve the contact surface of infected fluid with UVC evanescent zone of each element of composite material AS follows from the propagation of UVC radiation through the whispering gallery modes of big spherical/fiber elements permit the UVC radiation to penetrate a large distance inside the contaminated liquid and the contact of small elements with big one permits to diffuse this radiation in the volume of decontamination core.

This paper is constructed in the following way. In Sec. 2 we give the theoretical approach to the problem of decontamination proposing some possibilities of the repacking of small and big spheres (or thin and thick fibers) into decontamination core in order to win in the contact surface with UVC radiation which is propagated in this composite metamaterial. In Sec.3 it is proposed three experiments with repacked spheres, granulated material and repacked thin and thick fibers into the decontamination core of our equipment. This section contains the first repacking experimental results obtained with our equipment, in which is compared the decontamination efficiency of three methods of repacking of our decontamination tube under the action of UVC radiation. The theoretical and experimental results are in good concordance and help us to continue the upgrades and new possibilities of our equipment wining in the decontamination efficiency by improving the contact surface between infected fluid and the propagation of gallery modes of UVC radiation in each optical element of the metamaterial. Some correspondence between the theoretical prediction and experimental results is proposed using the statistical approach to experimental results.

Close Packing Possibilities of Elements of Metamaterial

In comparison with earlier proposed equipment, this report is focused on the applying of various geometry of packing elements of composite metamaterials like photon crystal in order to substantially increase the UVC decontamination contact surface with fluids and received an expected result for decontamination rate. We also propose the new more compact decontamination equipments for liquids and gases based on the idea of construction of composite metamaterials from micro- to nano-levels using the optical contact between synthesized metamaterial elements with various structural dimensions using repacking technologies. Here it is proposed to combine thick and thin elements of composite metamaterials formed from quartz spheres or optical fibre in order to achieve the expected results in decontamination efficiency. For this, we revised all packing structures formed by the balls/fibres, in the plane, Figure 1 and on the three dimension space, Figure 2. We are interested in to effectively utilized to remain free space between the big balls for disinfection procedures of contaminated fluids. This space may be expressed through the balls packing density in each metamaterial cell, where the cell density, depends on the packing structure of metamaterial. For example, in the hexagonal lattice arrangement this density is equal to which is larger than tetrahedral lattice packing one (see on the plan, Figures 1, and on in the space for homogeny packing structures, Figure 2). Taking

into consideration the efficiency of the decontamination contact surface between the elements of the periodical structures of metamaterials consisted from close packing quartz spheres and fibers described in our experiments [10, 11, 13, 15], we propose to use the combination of elements of metamaterials like spheres/fibers in the close packing procedure which form in principle the good material for the propagation of UVC radiation and contaminated liquids/gases penetration in it. For this, we revised all packing structures formed by the balls packing method. The free space between the big balls may be expressed through the atomic packing density in each metamaterial cell, $V_f = V(1-\rho)$, where the cell density, ρ , depends on the packing structure of metamaterial. For example, in the hexagonal lattice arrangement this density is equal to $\rho = \pi / (3\sqrt{3}) = 0.6086$ which is larger than tetrahedral lattice packing (see Figures 1 and 2), $\rho = \pi\sqrt{3}/16 = 0.3401$.

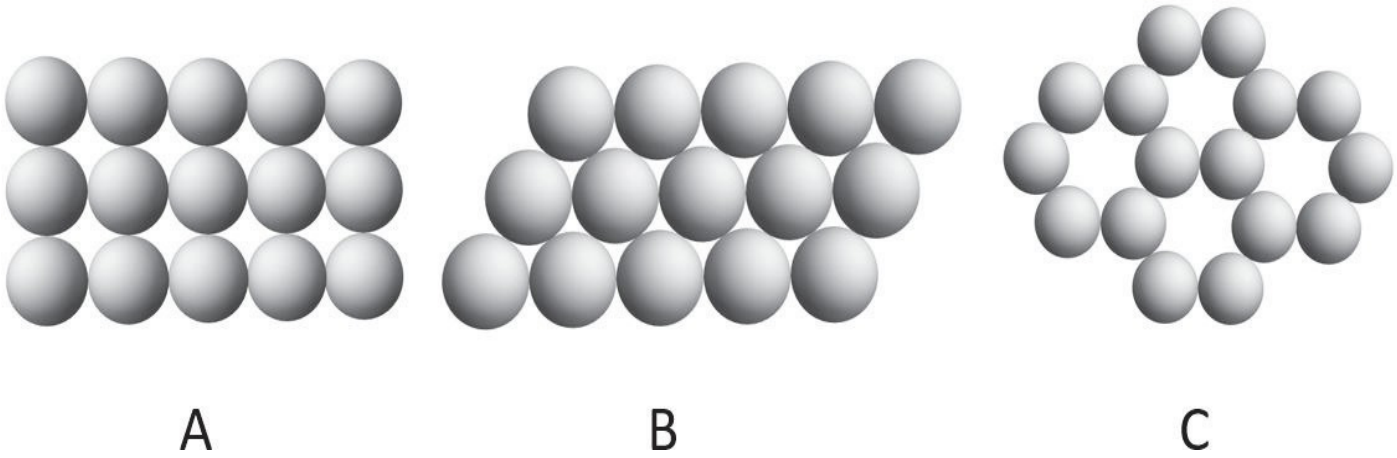

Figure 1: The close spheres (fibres) packing procedures on the plan: **(A)** square packing; **(B)** Hexagonal packing; **(C)** Basic hexagonal structure with some spheres is missing

The free volume in the above example is so that in tetragonal packing, we have more free space than in a hexagonal one. Following this example, we want to find the efficient decontamination volume which is proportional to the contact surface of the contaminated liquid with such packing balls multiplied to penetration depth of UVC radiation inside the fluid. Taking into consideration that the penetration depth, κ , on the free space between the balls is the proportional wavelength of radiation and inverse proportional to the difference between the refractive index of metamaterial, n_m , and contaminated fluid n_f , $\kappa \sim \lambda / [2\pi\sqrt{n_m^2 - n_f^2}]$, we can find this effective volume, $V_u = \kappa S$, where S is the contact surface of metamaterial with contaminated fluid. Let us demonstrate that this volume is smaller than the free volume between the balls, V_f . According to the relation between the surface of the ball and its diameter, d , we find the dependence between the total surface number of balls and their diameter, $S = \pi d^2 N$. Representing the number of the balls by N_l in the l direction of the space($l = x, y, z$) with the volume, $V = L_x L_y L_z$, filled up by the number of spheres in each direction $N_l = L_l / d$, it is easy to find the total number of spheres in the box $N = N_x N_y N_z$. This number is proportional to the volume $N \sim V / d^3$. Now the decontamination efficient volume around the ensemble of packing balls is proportional to the penetration depth, $\kappa \sim \lambda$, and inverse proportional to the diameter of the balls, $V_u \sim V\lambda / d$. Only for the small diameter of the balls, $d \sim \lambda$, can achieve the free volume between the balls described by the free volume V_f .

Let us propose the repacking procedure represented in Figure 3 in which the packing structures formed from the big balls represented in the Figures 1 and 2. In this situation, of course, we must found the resonances between the gallery modes of the waves in two balls with different diameters, as this is represented in Figure 3 by the spheres with the number "1" and "2". Not so larger estimations show us that for the ball diameters, $d \gg \lambda$, practically these resonances exist for the aleatory dimensions of the spheres, see Figure 3 C . It is represented right expresses the possible resonance between micro-resonators with different dimensions when the light wave can be considered standing wave (with its own quantum states) in both cavities with different dimensions. In this case, spheres with sub-micron dimensions are considered. This interaction can be also used between optical fibers of different thicknesses, respecting the conditions of guiding the waves through them.

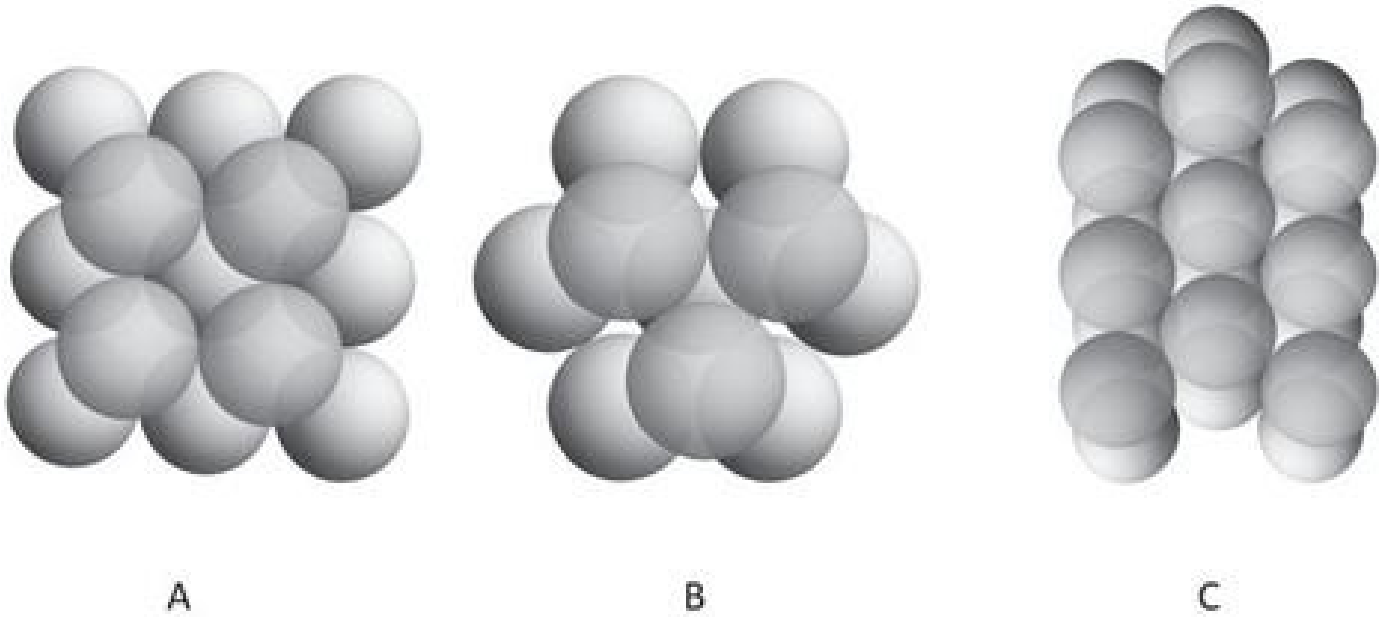

Figure 2: The hexagonal, tetrahedral and octahedral lattice arrangements of the quartz spheres in close packing

In order to win in the contact surface, we fill up the free space between the elements of metamaterial with other small elements. We observe that the total surface of i -species of balls, $S_i = 4\pi V_{fi} / d_i$, where $V_{fi} = V(1-\rho)^{(i-1)}$ is the free volume remain free volume after introducing the spheres with the dimension d_{i-1}. Here the diameter d_i of i -type of spheres is con In comparison with earlier proposed equipment, this paper is focused on the applying of various geometry of packing elements of composite metamaterials like photon crystal in order to substantially increase the UVC decontamination contact surface with fluids and received an expected result for decontamination rate. We also propose the new more compact decontamination for liquids and gases based on the idea of the construction of composite metamaterials from micro- to nano-levels using the optical contact between synthesized metamaterial elements with various structural dimensions using repacking technologies with the diameter of the $"i-1"$ sphere type by the relation $d_i = K^{-1}d_{i-1}$, here K^{-1} is ordered parameter less than unity. If we introduce a second 2 -types of spheres in the free space of cubic lattice, we obtain the following expression for the total surface $S = S_1 + S_2$. Here $S_1 = \pi d_1^2 N$ and $S_2 = \pi(\sqrt{3}-1)^2 d_1^2$ are the surface of the big and small spheres situate in the two lattices with the same number of nodes, N in optical contact. We not that the small spheres with diameter $d_2 = (\sqrt{3}-1)d_1$ are situated in the center of the cubes of the big one and don't have direct contact, where $K = 1/(\sqrt{3}-1)$. The total contact surface with contaminated fluid increases $S = \pi d_1^2 N(5-2\sqrt{3})$ with $0.56S_1$ relative, the metamaterial consisted of the packed spheres with the same diameter. We can continue to plot the small spheres in the cubic crystal. After the packing of the spheres in the center of the cube, we introduce the spheres in face of each cube's surface. For this, we estimate the distance between the small spheres with diameter $d_3 = d_1 - d_2$ and distance between four big spheres $d_3^* = d_1(\sqrt{2}-1)$. It observed that the diameter $d_3 = d_1(2-\sqrt{3}) \sim 0.28d_1$ is smaller than the diameter $d_3^* \sim 0.4d_1$. In this case, we can introduce the small sphere in the face of the cube with diameter $d_3 = d_1(2-\sqrt{3})$ which have tho optical contact only with spheres with diameter d_2 . It is not difficult to observe that such spheres are unstable in this packing configuration and can relax in four points of the free volume contacting the big spheres in the face. In this case the possibilities to obtain a stable periodic construction if we will introduce for the packing instead of the spheres the rotation ellipsoids with big and small diameters $(d_3^*, d_3) = (d_1(2-\sqrt{3}), d_1(2-\sqrt{3}))$. The total contact surface with fluids increases substantially to $S = S_1 + S_2 + S_3$ where for all elementary cell of the crystal we have three small spheres in the face of one cell $S_3 = 3\pi N d_3^2 = 3\pi N d_1(7-4\sqrt{3})$.

Similar conclusions may be done and for the packing procedure of the fibers with different diameters and the same length (see Figure 4). In this situation, the square packing of fiber with diameter d_1 permits the filing up the free space between them by fibers with the smaller diameter, $d_2 = d_1(\sqrt{2}-1)$, in the close packing procedure represented in Figure 4 A. The total surface of the fibers increases and becomes the sum of the thick and thin fibers $S_t = S_1 + S_2$. Here the total surface of the first or second fiber type is equal to the product of the perimeter of the circle multiply by their number and length, $S_i = \pi d_i L N_i$. For the thick fiber, we can find the relation

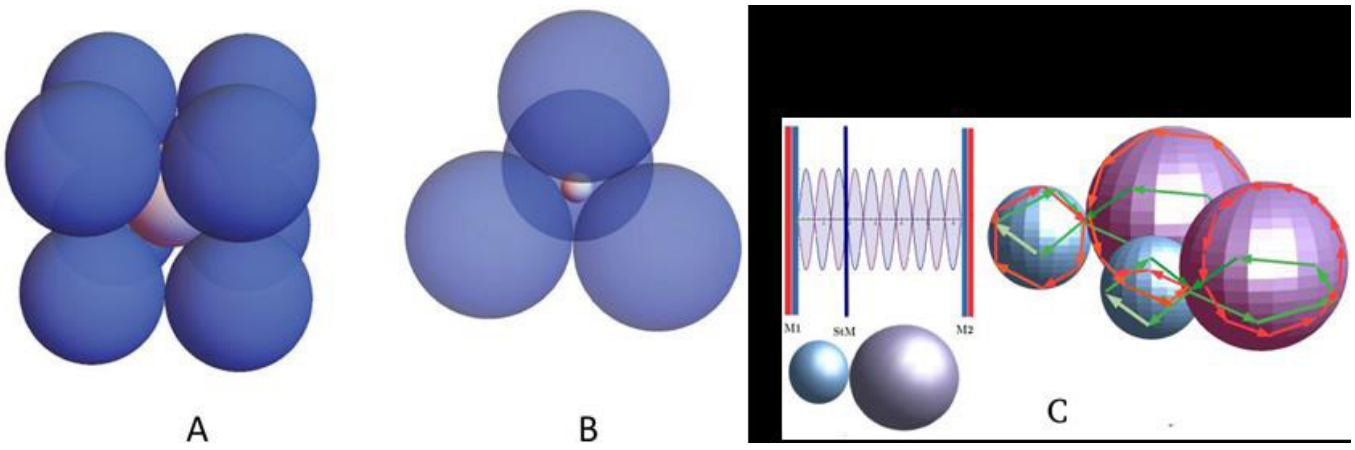

Figure 3: (A) The close packing of the small spheres between the big ones in cubic arrangement; **(B)** Packing the small spheres into the cells of the tetragonal lattice; **(C)** Optical resonances between the optical whispering-gallery modes belonging to the big and small spheres in repacking procedures

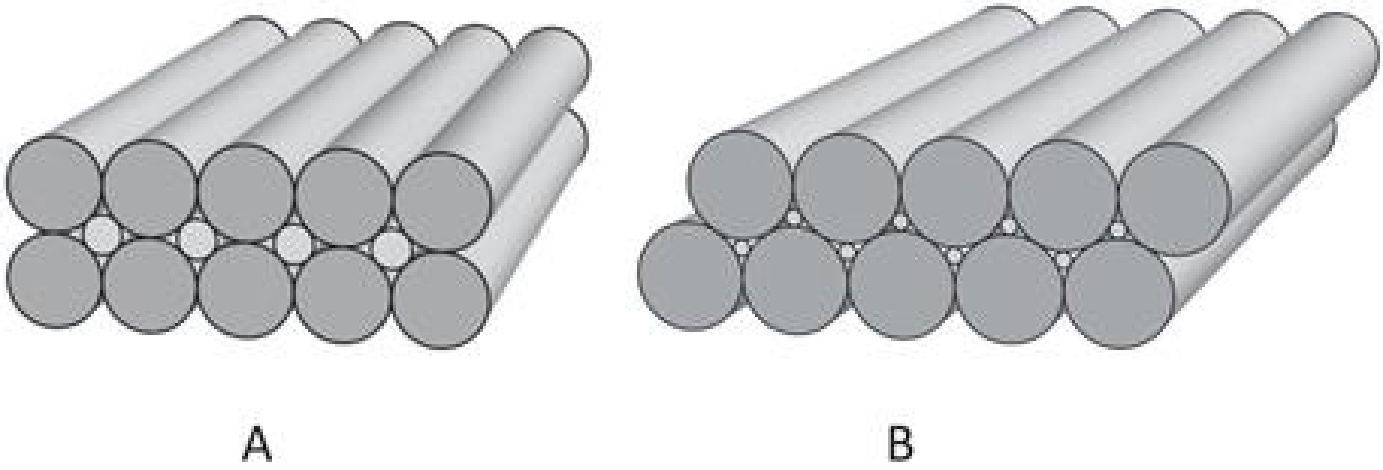

Figure 4: (A) The packing of two types of fiber in the square; **(B)** The hexagonal packing of two types of fibers

between their number, N_1 and diameters of the fibers, d_1 and d_2, and the dimension of the packing box, D, where these fibers are packed. Indeed, considering that these fibers filed up the square with length D we can easily approximate the side of the square by $D = N_x d_1$. As the square has the same number of fibers along the x and y sides, we can observe that $N_x = \sqrt{N_1}$, where $N_1 = N_x N_y$. In other words, the total surface of the packing fibers with the same diameter is $S_1 = \pi DL\sqrt{N_i}$. A similar conclusion may be obtained and by cylinder $S_i \sim DL\sqrt{N_1}$ which squeezes the unused space in the decontamination procedure of the fluids (see Refs. [10, 11, 15]). For thin fibers the estimations are similar with thick one $S_2 = \pi DL\sqrt{N_2}(\sqrt{2}-1) = S_1(\sqrt{2}-1)$. In the procedure of closed peaking of fibers, we obtain the win in the total decontamination surface with a value of about 0.44.

This procedure of close packing can be exported to the hexagonal arrangement of big fibers in the decontamination core represented in Figure 4B. In this situation, the radius of the introduced fibers is smaller than in square packing $r_2 = r_1(1-\sqrt{3}/2)$. The total surface consists of the surface of thin and thick fibers subsystems $S_t = S_1 + S_2 = 2\pi r_1(1-\sqrt{3}/2)LN$. Decontamination volume is proportional to this surface multiplied by the penetration depth of the UVC radiation.

We note that the crystalline packaging with smaller fibers/spheres has achieved an unstable construction. In this situation, to improve the decontamination rate, it is better to take the fibers/spheres with a diameter of $0,5-5\,\text{mm}$, smaller than the distance between the thick fibers (big spheres) and study the total contact surface with the contaminated fluid. If we consecutively pack the $"n"$ fibers/spe-

cies with the size of a smaller order, $K \gg 1$, in the free space between the spheres, we get the next improved total contact area, S_{tn}, with the contaminated fluid flowing by the metamaterial obtained. Taking into account the analytical expression for each type of the packing fibers/spheres, $S_i = t\pi V(1-\rho)^{i-1} / d_i$, we obtain the new relation for the total contact surface, $S_i = t\pi V(1-\rho)^{i-1} / d_i$, where $t = 4$ for spheres and $t = 1$ for fibers. The total surface of the composite assembly formed from "n" - types of fibes/balls becomes equal to the sum of the type of geometric progression sphere in the contaminated liquid we get next expression for total area $S_{tn} = \pi t V(1-q^n)/[d_1(1-q)]$, where $q = (1-\rho)K$. In the example above, $K = 10$. Maybe the situation in which the last term of the this expression gives the main contribution to the total surface of metamaterial. This is realized when the geometric progression ratio is larger than unity, $q \gg 1$. In this situation, the main contribution in total surface gives the aria with the smallest diameter. In this situation, $(1-\rho)K \gg 1$ the total area of composite metamaterial drastically increases with decreasing of diameter, $d_n = 10^{-(n-1)} d_1$, of the smallest packing fraction. But analytically expression takes into consideration and other situations in which for $K > 1$ and $(1-\rho) < 1$ is realized unity value of the geometrical progression ratio, $q = (1-\rho)K \sim 1$. In this situation, all species of quartz balls with diameter, $d_i = d_{i-1} / K$, give a substantial contribution to the composite metamaterial.

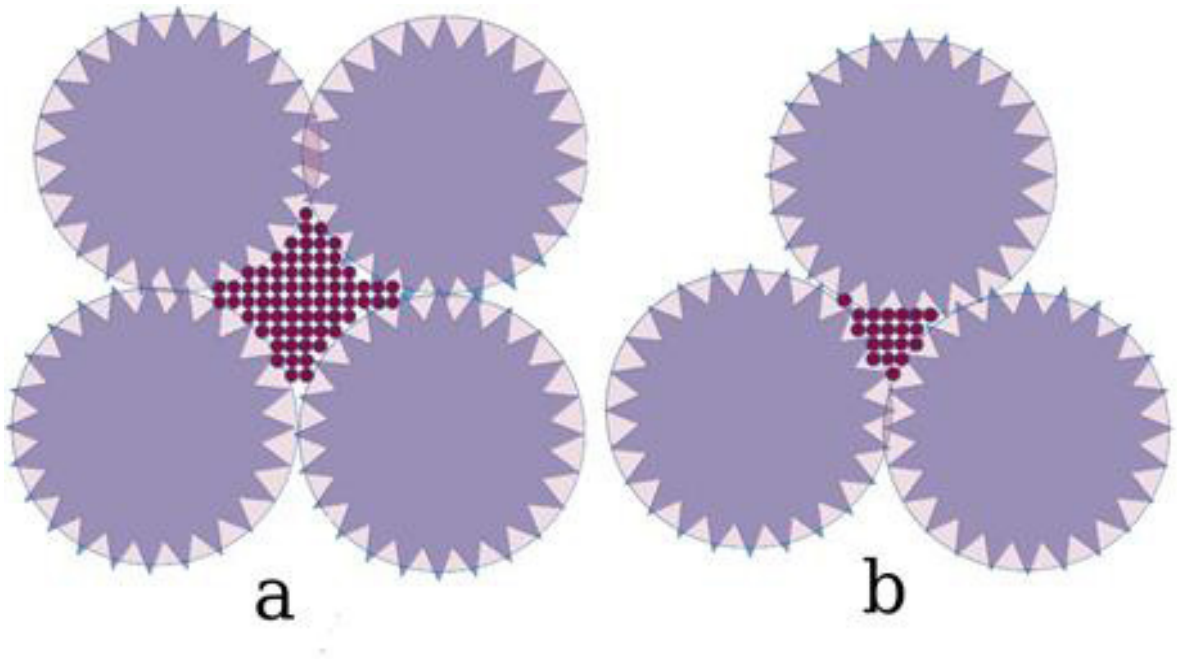

Figure 5: (A) The substitution of impenetrable space between the thick fibers with diameter d_1 filled up by thin fibers/spheres with diameter d_1 / K in square packing of the two types of elements; **(B)** The filled up of impenetrable space between the thick fibers (big spheres) by thin fibers (small spheres) in the hexagonal repacking with diameter $d_1 = d_1 / K$. The procedure of constraint of the impenetrable by radiation-free space can be continued till the packing of the smallest fibers/spheres with diameter $d_n = d / K^{n-1}$

In conclusion, we observe that the penetration of the UVC radiation inside the translucent fluids is an attractive problem from the decontamination point of view. To achieve this milestone in the composite metamaterials, we proposed to minimize the elements of periodical structures composed of spheres or fibers. This minimization of elements of metamaterial can not be continued till infinite. At first, glans apparently follows if we will drastically reduce the diameter of the quartz spherical elements or fiber elements of material, we can increase the contact surface and win in the decontamination rate. But this idea won't work for the necessity of deeper penetration of radiation inside the contamination fluids due to the existence of two inconvenient effects connected with the higher scattering of the UVC radiation on the surface of metamaterial elements formed from the quartz spheres/fiber with small diameters and increasing of the flow resistance of the liquid/gas inside the metamaterial. In this situation, the effective decontamination volume of metamaterial penetrated by contaminated fluid will be non-efficiently used. The laboratory observations demonstrate that the increase of the reflection from contact between the elements of metamaterials practically becomes an obstacle in the deeper penetration of radiation inside the fluid with the decreasing of the dimension of metamaterial elements. The combination of the big and small elements of metamaterial helps us to avoid the above obstacles.

Experimental Results

We substituted these contaminated fluids with pathogens with yeast solution, which has larger resistance to UVC radiation in comparison with many viruses or bacteria. The various dimension of yeast fungus colonies before going through the decontamination system tested in 12 probes represented in Figures 6. The mediation over the dimension and number of colonies was established on the number of probes, more than 20. These yeast solution samples are represented in Figure 6 in which we observed the aleatory dependence of colony dimension in each probe. With increasing the dimension, the number of colonies per same decreases. Our yeast solution belongs to Saccharomyces cerevisiae species with the proprieties to form the colonies. Formed from unicellular organisms and having the ability to be arranged in strings of connected budding the yeast cells known as pseudohyphae or false hyphae [21-27]. Life within these populations is a prevalent form of microbial existence in natural settings that provides the cells with capabilities to effectively defend against environmental attacks as well as efficiently adapt and survive long periods of starvation and other stresses. As a eukaryotic cellular construction, the yeast colonies oppose more large resistance to UVC radiation in comparison with the pathogen prokaryotic cellular colonies. Yeast sizes achieved the dimension $1-30\mu m$ in diameter and present an interest to study the evolution of the number of yeast colonies before and after the decontamination procedure. For this, we propose to use the normal distribution [28,29] of yeast colony relative to their number $(1/\sqrt{2\pi\sigma_n})exp[-(n-n_0)^2/(2\sigma_n^2)]$, and their diameters, $(1/\sqrt{2\pi\sigma_{d_n}^2})exp\left[-(d_n-d_{n_0})^2)/(2\sigma_{d_n}^2)\right]$. Here n is the number of colonies in each microscopical tests in which the dimensions d_n is also described by normal distribution; $\sigma_{d_n}^2$ is the standard deviation from mean value the size d_{n_0}, and σ_n is the fluctuation of number of yeast colonies for their mean number n_0. The application of the normal distribution in such experimental measurements follows from the conditions discussed in the Ref. [29]. From our experimental results, we estimate the average prepared for decontamination of yeast solution. Before deactivation, we have $n_0 = 9$; $\sigma_n = 2$; $d_{0n}/d_{sp} = 0.05/n_0$ and $\sigma_{d_n} = 0,1/d_{sp}$. Here d_{sp} is the visualized diameter of the microscope image represented in Figure 6.

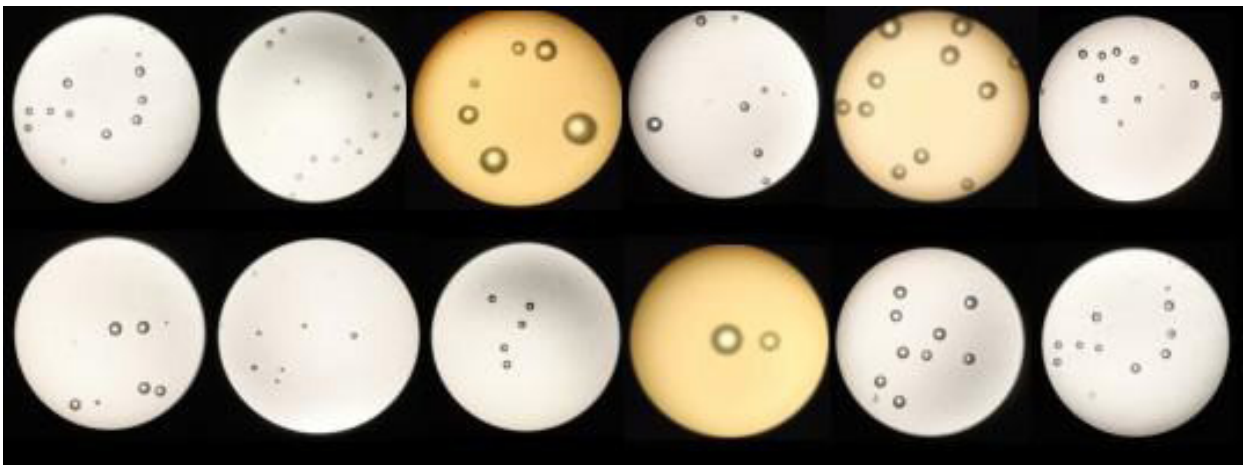

Figure 6: The various dimension of yeast fungus colonies before going through the decontamination system tested in the 12 probes. The mediation over the dimension and number of colonies was established than 20 probes. The 12 probes are represented in this figure. It is observed the dependence of colony dimension as the function of its number on the probe. With increasing the dimension the number of colonies per same decreases

Experimentally observations represented have shown that a big part of liquid flows is well decontaminated during the time less than $t = 5min$. In Figures 7 we proposed three types of repacked metamaterials used in the decontamination core of the equipment represented in Figures 8. As is shown the Figures 6 dimensions become smaller than the initial one and many of them were destroyed (about $70-80\%$). In order to demonstrate that filling up the space between the elements of metamaterial play an important role, it is proposed in another experiment which are involved thin and thick fibers or big and small bubbles. In these situations, the big space between the quartz granules is filled up by small ones, so that radiation non-penetrated free space decreases. This reduction of the space between the elements of metamaterial demonstrates that the decontamination rate increases. This is in accordance with the

theoretical prediction proposed in Section 2. In the experimental situation represented in Figure 7B, the mixture of the granulated quartz material with large dispersion in the mean value of the granule dimension (from 0.01 cm to $0.5cm$) demonstrates the big decontamination rate in comparison with the bubbles/fiber system represented in Figures 7A or C. The simple explanation of this effect consists in the fact that the size of the granules allows the radiation to be directed to the center of the tube with a diameter of about $3.0cm$.

According to our theoretical discussion in section 2, we may put three experiments with such metamaterials represented in Figures 7. Two experiments contain the system of quartz balls with the dimensions $d_1 \sim 1-2\,mm$ and fibers with diameter about $d = 1mm$. Another experiment contains crushed granulated quartz material represented in Figure 9 B. Here we have compared the contact surface of the quartz spheres and fiber optics system. The granulated quartz metamaterial with various dimension is proposed for an experiment in which in our opinion is realized the situation in which between the big elements are introduced the smaller elements of the composite metamaterial so that the total surface can be approximated by the sum of the surfaces of elements with the same optical characteristics $S_t = S_1 + S_2 + S_3 + ...S_n$. The quality of decontamination depends on the method of granulating the quartz balk during crushing. This effect was established during the measurements. All three types of metamaterials were introduced in the decontamination core, which consists of a quartz tube with a length of 100 cm and a thickness of about $3.$ cm.

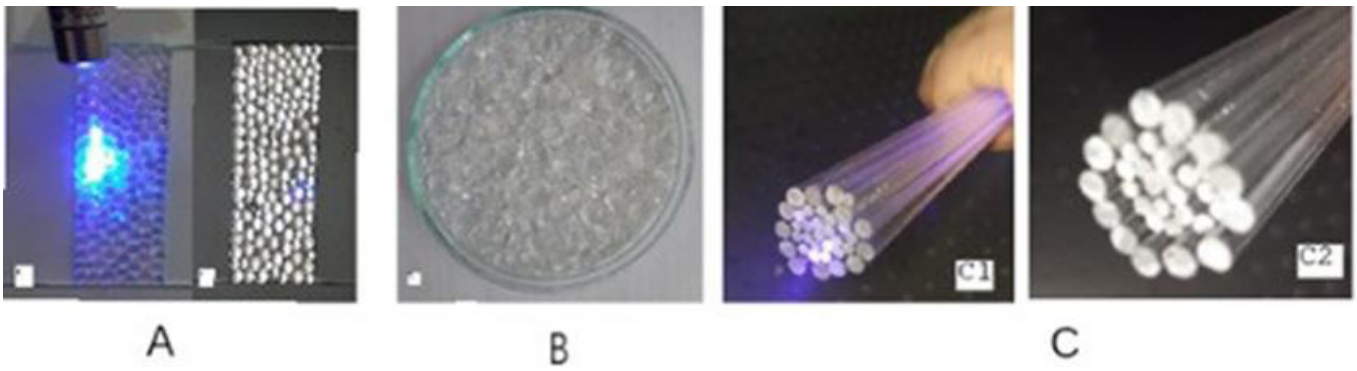

Figure 7: $1A$ corresponds to the blue laser radiation of the sample and $2A$ without blue laser radiation and decontamination results plotted in Figure 9. Figure B corresponds to the metamaterials formed from dropped quartz with different dimensions from 10^{-5} mm to $1-2$ mm. Figure C represents the two-type of optical fibers repacked in the decontamination of the core of the equipment so that the free space between them achieved minimal value. The decontamination results for this metamaterials are plotted in Figure 9.

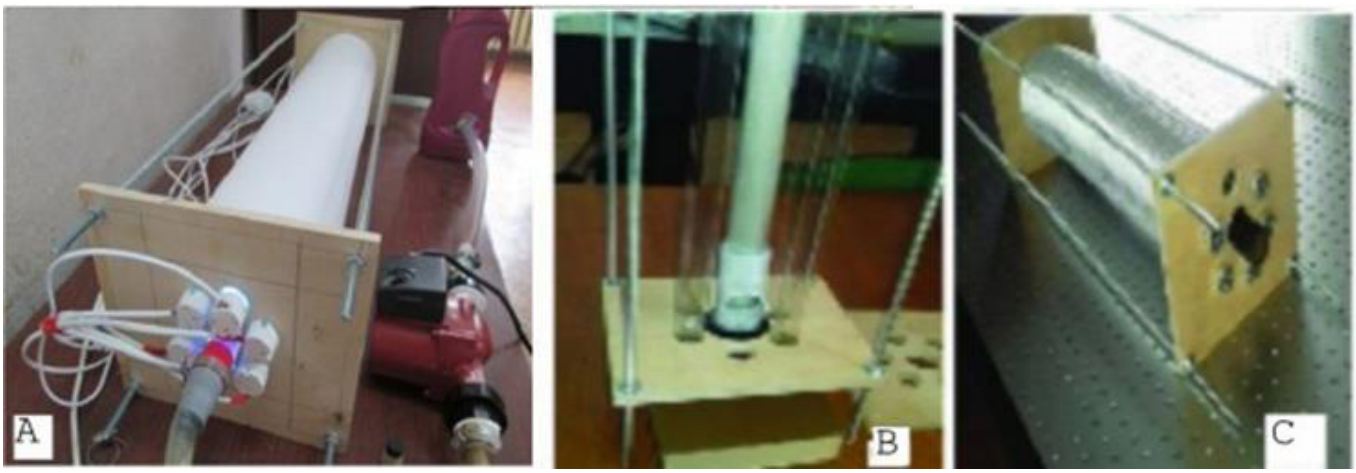

Figure 8: The decontamination core filled up by metamaterials described Figure 6. In the figure, A, we represent the core radiated by 6 UVC lamps. All system of lamps and decontamination the core is introduced in the big aluminum cylinder with diameters about $15-20$ cm, which protects us from the environment UVC radiation and substantially focuses the possible losses of radiation inside the center of the big cylinder where it is situated the decontamination core.

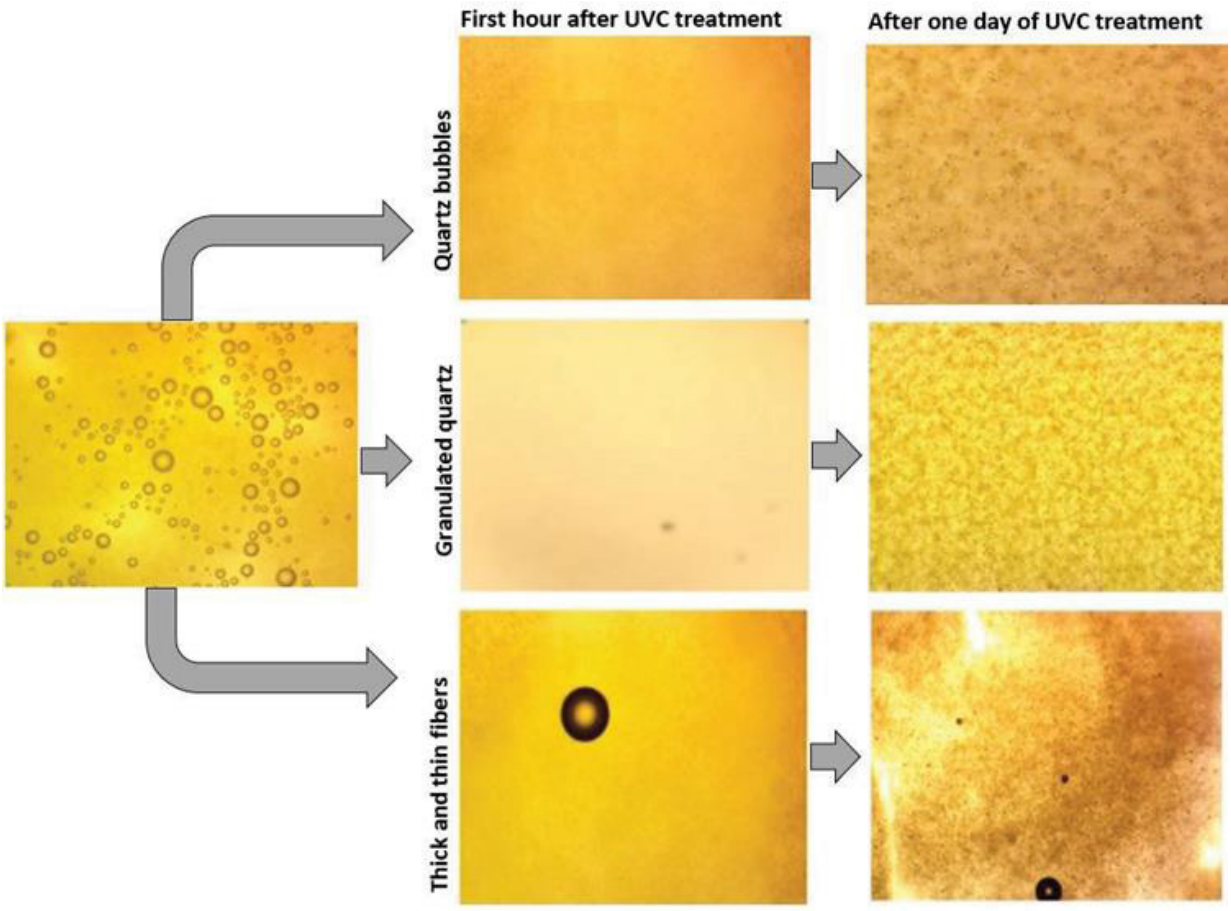

Figure 9: The UVC decontamination using different types of metamaterials, quartz balls, granulated quartz, thick and thin fibers

The two types of quartz bubbles were packed in the core of the equipment represented in Figure 7. After $5min$ of decontamination time interval the big number of yeast colonies were inactivated (see Figure 9). In order to compare this metamaterial with quartz granules, we give the remaining yeast small fungus to increase during the 24 hours. This method gives us the possibility to estimate the decontamination rate of three types of material described in Figures 7 A, B, and C.

The role of the small granules in the optical contact with the large one scattered the standing waves in the non-penetrating UVC radiation in the free space between the large granules. The yeast solution flowing through such space can efficiently decontaminate the pathogen with the metamaterial formed from repacking fibers/spheres represented in Figure 9. From the experiments observed there is a noticeable substantial decrease in the radius of fungus colonies and their number in the case of repacking model. In composite granulated metamaterial with the same spheres represented in Figure 9, we observed the relative higher decontamination rate under the same exposure time and the same concentration of fungus colonies used in the fiber system. Microscope visualization demonstrates that if we introduce only big balls with the $3mm$ in diameter in the decontamination core the total decontamination is achieved in $8-10min$ in comparison with repacking one.

Let us comment and an experiment with quarts fibers, which consisted of a $3.0\,cm$ diameter quartz tube filled up with $2\,mm$ and $1\,mm$ in diameter two types of quartz fibers. The decontamination volume is larger than the free volume between the homogeneous packed fibers with the same big diameter of about, $2\,mm$, due to the repacking method proposed Sec. 2. The repacking of the fiber demonstrates the same improvement of decontamination time which is inversely proportional to the contact surface ($5min$ less than with homogeneous fiber systems with diameter $2\,mm$ in which is observed about $10min$ decontamination time).

According to the experimental results represented in Figure 9 the good decontamination was obtained with granulated metamaterial. Not so bad decontamination rate in comparison with quartz granules was obtained with two types of packing bubbles/fibers. In these experiments, we don't have exactly the situation proposed in the theoretical conception of close packing spheres/fibers. But of course, the granulated material represents more plotted metamaterial and the decontamination volume of evanescent zones around the elements is larger than in two types of bubble packing. The two types of fiber systems were radiated perpendicular to the fibers. The yeast solution flows laminar between the fibers so that a lot of fungus colonies remain in the non-penetration space by UVC radiation. This may be the explanation for not so well decontamination rate. Here we don't use the fibers with a diameter less than $5-10$ times smaller than the thick fibers. This also is an argument on not so good decontamination rate in comparison with bubbles and granulated material.

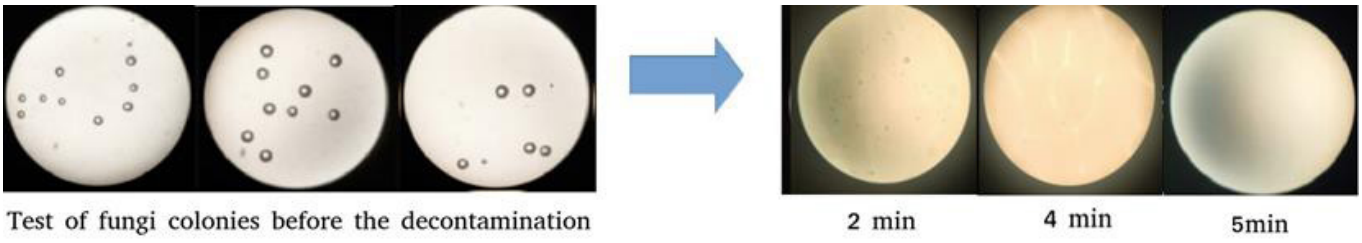

Figure 10: We represent the yeast fungus before going through the decontamination system. The mediation on the number and dimensions of colonies observed on the 25 experiments was about 5 per picture. The yeast fungus after it has gone through the decontamination system filled with a mixture of the granulated quartz, After $4-5\ min$ is observed the good inactivation.

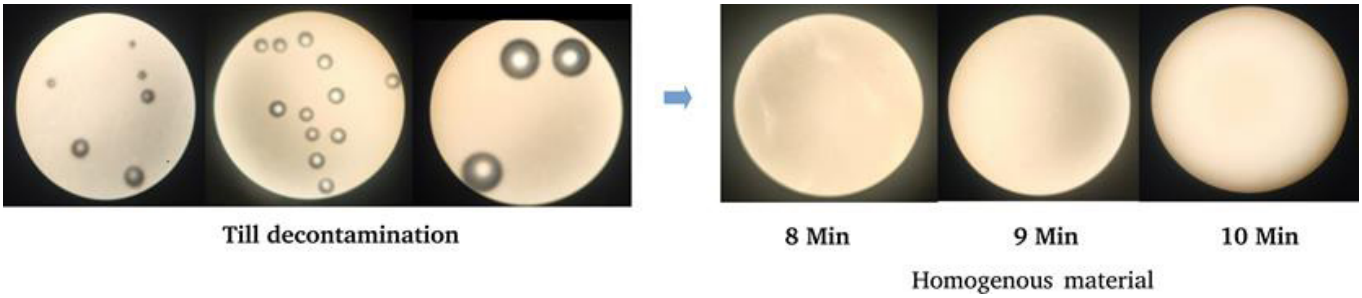

Figure 11: Approximate the same preparation of yeast fungus for homogeneous packing of big bobbles with the same diameter, $3\ mm$, in which about $8-10\ min$ are necessary for decontamination.

As the granulated material is more effective than the spherical one and fibers repacking, we have used it for the establishment of the decontamination statics during of fungus number and their dimension as a function of the time flowing through the granules of such metamaterial. We have three exposition times of this flow $t = 2\ min$ and $t = 4\ \ min$ and 5 min (see Figures 10). For deactivation time equal to $5\ min$ practically the fungus is not observed in our optical microscope. For flow time $t = 2\ min$, the decontamination rate demonstrates that the mean number of fungus colonies on the visualization area of the microscope is 4 times smaller than in the initial pictograms, and the mean dimension decreases with the same value. This result is compared with homogeneous metamaterial formed from 3 mm bubbles in which the same inactivation is being more later, $8-10\ min$ (see Figure 11).

Conclusions

The proposed repacking method of transparent elements of optical material describes how to use non-penetrated space inside the metamaterial for improving the decontamination efficiency through the addition surface. The repacking of periodical structures with other elements is specific for a lot of effects existing in multiple complex crystals and glass structures [30] and it is observed its functional roles in multiple proteins in which such complexes as tubulins play a specific role in living cells [31-33]. In this paper, we have proposed the idea of how to use the space between big and elements of one composite metamaterial for improving contact between the UVC radiation and fluid repacking this space in close contact with the big one. The new equipment may be used as a method of decontamination of nontransparent fluids in UVC frequency interval. The multiple reflections of radiation inside the metamaterial

and proposed aluminum box give us possibilities to improve the decontamination rate of decontamination equipment applying it in the different conditions and for various fluids including aerosols in the living rooms and non-transparent infected with viruses and bacteria nanoparticles in water.

The combination of small and large elements of metamaterial opens the new opportunity of establishing the optical connection between the big elements and pathogens from the fluid through the small granules of the proposed composites. The resonance penetration of radiation from one granule to another with smaller order can be used in the transmission of UVC radiation to bio-molecular tissue of living cells, in which the exact channelization of radiation in the small regions of photo-transformation reactions which in many cases is not so well understood. The comparison of contact volume of these metamaterials with existing method of decontamination may be easily understood if we observe that the total decontamination volume is area proportional to the surface of core cylinder multiplied to the penetration deeps. The last disinfection volume is substantially smaller than the decontamination volume of metamaterial introduced in the core. It includes the same surface volume of the big cylinder plus the additional volume represented by the sum of the surface of each element of metamaterial (sphere/fibres). The last volume is proportional to the $\sqrt{N}$ of the number of metamaterials, and drastically increases in comparison with surface volume of the big cylinder, when the dimensions of the spheres decrease.

The proposed equipment contains the closed chamber represented by the big cylinder with diameter 200 mm and length about $1\ m$, which not only protect the people from the room by UVC radiation, but it construction from good reflection material like aluminium coating (see Figure 8). Focused radiation in the centre of decontamination drastically amplifies the radiation in the decontamination core volume due to multiple reflections from aluminium coating. These two priorities of proposed equipment can be used in populated place (hospitals, airports, living, etc.), due to the closed radiation inside the decontaminator. For comparison to traditional method of UVC decontamination systems, in which the people must leave the working place during the disinfection time, the new equipment not only eliminate this, but multiple reflections of radiation inside the decontamination cylinder permit us to use effectively the quantity of emission UVC radiation from the sources. In order to increase the quantity of treated fluids, it is possible to utilize such equipment in parallel connection, one on top of the other, under the pumping of infected water or aerosols in air.

Acknowledgment

This paper is supported by the projects: ANCD 20.80009.5007.01 and NATO EAP SFPP 984890.

References

1. Dai T, Vrahas MS, Murray CK, Hamblin1 MR (2012) Ultraviolet C irradiation: an alternative antimicrobial approach tolocalized infections? Expert Rev Anti Infect Ther 10: 185-95.

2. Sabino CP, Ballc AR, Baptistad MS, Daief T, Hamblineg MR, et al. (2020) Light-based technologies for management of COVID-19 pandemic crisis. J Photochem Photobiol B 212: 111999.

3. Heling M, Hnes K, Vatter Petra, Lingenfelder C (2020) Ultraviolet irradiationdosesfor coronavirus inactivation-review and analysisof coronavirus photoinactivationstudies GMS GMS Hyg Infect Control 15: 10.3205/dgkh000343.

4. Kalyani VL, Laxmi V, Prachi K, Prachi M, Nupur M, et al. (2020) Study on Coronavirus (COVID-19) and how UVC Light helps to Destroy it and its Applications. Journal of Management Engineering and Information Technology (JMEIT) 7: 10.5281/zenodo.3929714.

5. Buonanno M, Welch D, Shuryak I, David J (2020) Far-UVC light (222 nm) efficiently and safely inactivates airborne human coronaviruses, Sci Rep 10 10285.

6. Mack R (2020) Covid-19 and fiber optic cable assemblies FOC News.

7. Baer TM, Baer CE (2020) Optics and the COVID-19 Pandemic Optics & Photonics News.

8. Perepechkin LP, Perepechkina NP (1999) Hollow fibres for medical applications. A review. Fibre Chemistry 31: 411-20.

9. Cadwell JJS (2015) The Hollow Fiber Infection Model: Principles and Practice Adv Antibiotics Antibodies 1: 1.

10. Enaki NA, Profir A, Ciobanu N, Bazgan S, Nistreanu A, et al. (2017) Optical metamaterials for decon-tamination of translucent liquids and gases. J Phys D 51: 385101-11.

11. Enaki NA, Bazgan S, Ciobanu N, Turcan M, Paslari T, et al. (2017) Improvement in ultraviolet based decontamination rate using meta-materials. Applied Surfaace Science 417: 40-7.

12. Cadwell JJS (2017) The hollow fiber infection model: Principles and practice Arch Clin Microbiol 8: 5.

13. Enaki NA, Profir A, Bizgan S, Paslari T, Ristoscu C, et al. (2017) Metamaterials for Antimicrobial Biofilm Applications: Photonic Crystals of Microspheresand Optical Fibers for Decontamination of Liquids and Gases Handbook of Antimicrobial Coatings Elsevier 13-27.

14. Annamdas VGM, Soh KCh (2019) A Perspective of Non-Fiber-Optical Metamaterial and Piezoelectric Material Sensing in Automated Structural Health Monitoring Sensors 19: 1490.

15. Enaki NA, Bazgan S, Nistreanu A, Tonu V, Turcan M, et al. (2018) Efficient microbial decontamination of translucent liquids and gases using optical metamaterials In the book: Advanced Surface Engineering Research IntechOpen 9: 169-97.

16. Williams JC (1970) The properties of non-random mixtures of solid particles. In the book: Powder Technology, InTechOpen 3: 189-194.

17. Capolino F (2009) Theory and Phenomena of Metamaterials. Metamaterials Handbook Taylor & Francis 10.1201/9781420054262.

18. Baas AF, Tretyakov Sergei, Barois P, Scharf T, Kruglyak V, et al. (2010) Nanostructured Metamaterials: Exchange between experts in electromagnetics and material science Editor in Chief EUROPEAN COMMISSION.

19. Tadesse AD, Acharya OP, Sahu S (2020) Application of metamaterials for performance enhancement of planar antennas Int J RF Microw Comput Aided Eng 30: e22154.

20. Surjadi JU, Gao L, Du H, Li X, Xiong X, et al. (2019) Mechanical Metamaterials and Their Engineering Applications Adv Eng Mater 21: 1800864.

21. Yong E (2012) Yeast suggests speedy start for multicellular life Nature News Springer Nature 10.1038/nature.2012.9810.S2CID 84392827.

22. Ratcliff WC, Denison RF, Borrello M, Travisano M (2012) Experimental evolution of multicellularity Proc. Natl Acad. Sci. USA 10.1073/pnas.1115323109.

23. Boraas ME, Seale DB, Boxhorn JE (1998) Phagotrophy by a flagellate selects for colonial prey: A possible origin of multicellularity Evolutionary Ecology 12: 153-64.

24. Koschwanez JH, Foster KR, Murray AW (2011) Sucrose utilization in budding yeast as a model for the origin of undifferentiated multicellularity. PLoS Biol 9: 10:e1001122.

25. Rosa CA, Gbor P (2006) Biodiversity and Ecophysiology of Yeasts Series: The Yeast Handbook, Springer, USA.

26. Walkeellipser K, Skelton H, Smith K (2002) Cutaneous lesions showing giant yeast forms of Blastomyces dermatitidis. Journal of Cutaneous Pathology 29: 616-8.

27. Legras JL, Merdinoglu D, Cornuet JM, Karst F (2007) Bread, beer and wine: Saccharomyces cerevisiae diversity reflects human history. Molecular Ecology 16: 10.

28. Weisstein EW (2020) Normal Distribution. mathworld.wolfram.com. Retrieved August 15.

29. Lyon A (2014) Why are Normal Distributions Normal? Brit J Phil Sci 65: 621-49.

30. Barry Carter C, Grant Norton MM (2013) Complex Crystal and Glass Structures In: Ceramic Materials, Springer Science+Business Media New York, USA.

31. Binarová P, Tuszynski J (2019) Tubulin: Structure, Functions and Roles in Disease. Cells 8: 1294.

32. Barbier P, Zejneli O, Martinho M, Lasorsa A, Belle V, et al. (2019) Role of Tau as a Microtubule-Associated Protein: Structural and Functional Aspects. Front Aging Neurosci 11: 204.

33. Berman GP, Nesterov AI, Liopez GV, Sayre RT (2015) Superradiance Transition and Nonphotochemical Quenching in Photosynthetic Complexes. J Phys Chem C 119: 22289-96.